The orderly allocation of mesodermal cells to the extraembryonic structures and the anteroposterior axis during gastrulation of the mouse embryo

Simon J. Kinder[1], Tania E. Tsang[1], Gabriel A. Quinlan[1], Anna-Katerina Hadjantonakis[2], Andras Nagy[2] and Patrick P. L. Tam[1,*]

[1]Embryology Unit, Children's Medical Research Institute, Locked Bag 23, Wentworthville, NSW 2145, Australia
[2]Samuel Lunenfeld Research Institute, Mount Sinai Hospital, 600 University Avenue, Toronto, Ontario M5G 1X5, Canada
*Author for correspondence (e-mail: ptam@cmri.usyd.edu.au)

SUMMARY

The prospective fate of cells in the primitive streak was examined at early, mid and late stages of mouse gastrula development to determine the order of allocation of primitive streak cells to the mesoderm of the extraembryonic membranes and to the fetal tissues. At the early-streak stage, primitive streak cells contribute predominantly to tissues of the extraembryonic mesoderm as previously found. However, a surprising observation is that the erythropoietic precursors of the yolk sac emerge earlier than the bulk of the vitelline endothelium, which is formed continuously throughout gastrula development. This may suggest that the erythropoietic and the endothelial cell lineages may arise independently of one another. Furthermore, the extraembryonic mesoderm that is localized to the anterior and chorionic side of the yolk sac is recruited ahead of that destined for the posterior and amnionic side. For the mesodermal derivatives in the embryo, those destined for the rostral structures such as heart and forebrain mesoderm ingress through the primitive streak early during a narrow window of development. They are then followed by those for the rest of the cranial mesoderm and lastly the paraxial and lateral mesoderm of the trunk. Results of this study, which represent snapshots of the types of precursor cells in the primitive streak, have provided a better delineation of the timing of allocation of the various mesodermal lineages to specific compartments in the extraembryonic membranes and different locations in the embryonic anteroposterior axis.

Key words: Primitive streak, Cell fate, Mesoderm, Gastrulation, Mouse

INTRODUCTION

During mouse gastrulation, cells recruited from the epiblast ingress through the primitive streak (PS) and are organized into layers of mesodermal cells that constitute the embryonic and extraembryonic mesoderm. Although the formation of the mesoderm has been extensively studied (Hashimoto et al., 1987, Lawson et al., 1991; Lawson and Pedersen, 1992a,b; Parameswaran and Tam, 1995; Tam and Beddington, 1987; Tam et al., 1993, 1997), little is known about the morphogenetic processes that influence the placement of mesodermal cells in different parts of the embryonic axis and the extraembryonic membrane. Fate-mapping studies of the mesoderm of the gastrulating embryo reveal that cells that are destined for the extraembryonic mesoderm constitute the major tissue type in the nascent mesodermal layer. The precursors for cranial and heart mesoderm are present later in the mesodermal layer of the mid-streak stage embryo, but are ahead of those that contribute to the paraxial and lateral mesoderm of the trunk, which form the bulk of the embryonic mesoderm in the late-streak embryo (Parameswaran and Tam, 1995; Tam et al., 1997). These studies also show that the various mesoderm precursors are distinctly regionalized in the mesodermal germ layer and their relative position is concordant with the final location in the fetal body. An examination of the regional distribution of PS-derived cells in the paraxial mesoderm has revealed that PS cells are allocated to the somites in a craniocaudal manner (Tam and Beddington, 1987). Epiblast cells that are recruited to the PS at successive stages of gastrulation are also found to be distributed similarly in a craniocaudal order to the gut endoderm (Tam and Beddington, 1992; Lawson et al., 1987; Lawson and Pedersen, 1986).

During gastrulation, cells in the epiblast and their descendants are progressively displaced towards the PS where cellular ingression takes place (Lawson et al., 1991; Lawson and Pedersen, 1992a). It is possible that cells in the epiblast are recruited for ingression in a sequential order that is determined by their geographic proximity to the PS. This may imply that the position of the cells in the epiblast predisposes the order and timing of their recruitment and thus their destination in the anteroposterior axis of the body plan. However, clonal analysis of epiblast cells has revealed significant overlap in the distribution in both the ectoderm and the mesoderm along the anteroposterior body axis of clones arising from cells localized in different regions of the epiblast (Lawson et al., 1991; Lawson and Pedersen, 1992b). Indeed, any spatial restriction of clonal

populations that may have been established in the epiblast of the peri-implantation embryo would have been lost during the extensive intermingling of cells in the epiblast before and during gastrulation (Gardner and Cockroft, 1998; Lawson et al., 1991). It is therefore unlikely that any pre-existing pattern of spatial allocation can be maintained during the morphogenetic movement of epiblast cells as they are recruited to the PS. In essence, the location of the cells in the epiblast does not predict the destination of their descendants and there is no compelling evidence that any anteroposterior pattern is established in the epiblast population (Lawson and Pedersen, 1992a,b). The lack of spatial restriction of clonal populations in the epiblast implies that if the regionalization of cell fate in the mesoderm and endoderm layer is indeed indicative of some order of allocation of the embryonic tissues to the body plan, then the patterning or ordering mechanism must be established during the transit of epiblast-derived cells at the PS. This is the main issue addressed by the present fate-mapping study of the cells in the PS.

Establishment of the extraembryonic blood circulation during gastrulation is an essential factor in embryonic survival. The formation of the first blood cells occurs in the blood islands of the yolk sac mesoderm and is known as primitive erythropoiesis. The concomitant development of the vascular endothelium of the yolk sac, allantois and embryo proper allows the development of the blood circulation. It is believed that the extraembryonic mesodermal cells destined to become erythropoietic cells and vitelline endothelium are descendants of a common precursor aptly named the haemangioblast (Nishikawa et al., 1998). Precursors of the extraembryonic mesoderm are located in the proximal epiblast and are the earliest mesoderm to migrate through the streak (Lawson et al., 1991). The present study therefore attempts to find out if cells in the proximal epiblast and the PS may contribute to both cell lineages in the extraembryonic mesoderm during gastrulation.

The present study was performed to address three issues raised by the above data. (1) Does the timing of transit of cells through the PS correlate with the localization of the mesodermal derivatives in the anteroposterior axis of the embryo? (2) Does this rule apply similarly to the distribution of mesodermal cells to different compartments of the extraembryonic structures? (3) Do the progenitors of the erythropoietic cells pass through the streak at the same time as those of the vitelline endothelium, which may denote the possibility of a common lineage?

MATERIALS AND METHODS

Experimental strategy

The developmental fate of cells in the primitive streak (PS) of early primitive streak (ES), mid-primitive streak (MS) and pre- to early-bud (0B/EB)-stage embryos (Fig. 1) was tested by orthotopic transplantation of *lacZ*- or GFP-expressing transgenic cells and in situ labeling of cell populations. The micromanipulated embryos were examined after 24-48 hours of in vitro culture to determine the localization and number of transgenic or labeled cells in different tissues at the whole embryo and histological level (Tables 1, 2).

Cells at different sites in the PS were studied for their developmental fates. At ES stage only one PS site (P1) in the most posterior proximal egg cylinder was tested. In addition, cells at site A in the anterior proximal epiblast, which later will be recruited to the posterior PS during gastrulation (Lawson et al., 1991), were tested by

orthotopic transplantation (Fig. 2A). At the MS-stage, sites in the most proximal (P2), the mid (P3) and the most distal segment (P4) of the PS were studied (Fig. 3A). At the 0B/EB stage, four sites were examined (Fig. 4A). From proximal to distal, these sites are located at the most proximal (P5), at 1/3 of the length from the proximal end (P6), at 1/2 way along the streak (P7) and at 3/4 of the length of the streak from the proximal end (P8). Transplanted or labeled embryos were cultured until they reached the early-somite stage and were then examined for tissue colonization by the transplanted cells or the distribution of labeled cells.

Dissection, micromanipulation and culture of embryos

Pregnant mice were dissected at 6.5 days post coitum (dpc), 7.0 dpc and 7.5 dpc to yield embryos of ES stage, MS stage and 0B/EB stage (Downs and Davies, 1993), respectively. Two strains of mice expressing respectively the *HMG-CoA-lacZ* (denoted as the H253 strain: Tam and Tan, 1992) and the *β-actin-CMV-EGFP* (the B5/EGFP strain: Hadjantonakis et al., 1998) transgenes provided the donor embryos. Stage-matched ARC/s strain embryos were used as recipients.
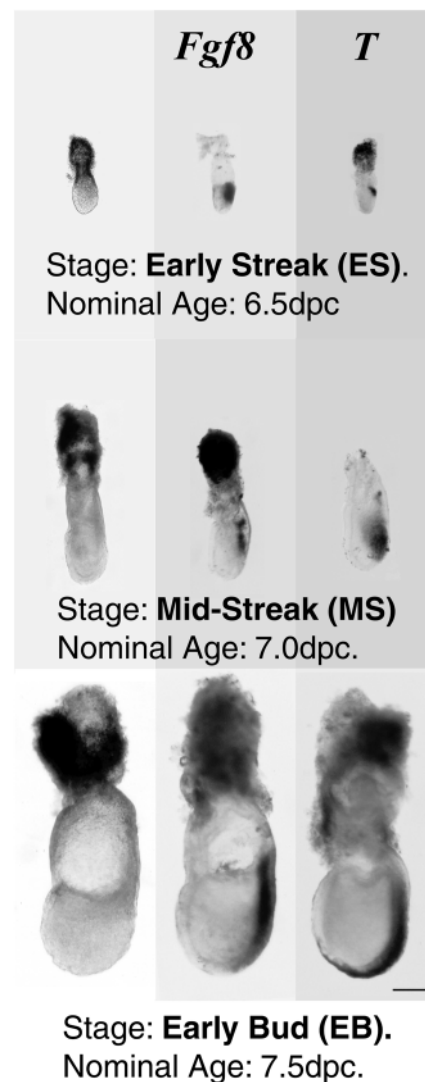
Fig. 1. Mouse embryos used for fate-mapping experiments at early streak (ES), mid-streak (MS) and early bud (EB) stages (Downs and Davies, 1993). The development of the PS is revealed by the expression pattern of *Fgf8* and *Brachyury* genes. Scale bar, 200 μm.

Donor embryos were dissected using fine glass needles (Sturm and Tam, 1993) to obtain tissue fragments from various regions of the PS (see Figs 2-4). At ES stage, tissue fragments were also isolated from the anterior lateral epiblast region of the embryo (see Fig. 2A). The fragments were further dissected first to remove any adherent visceral endoderm and then to obtain clumps of 5-10 cells for transplantation. Cell clumps were grafted orthotopically into recipient embryos using a Leitz micromanipulator under a dissecting microscope (Wild M3Z) or a Leica Fluorovert inverted microscope (Kinder et al., 1999). After grafting, embryos were incubated for 1 hour in either DR75 (75% rat serum and 25% DMEM, Sturm and Tam, 1993) culture medium (0B/EB stage) or 100% rat serum (MS and ES stages) in static culture to allow graft to integrate. ES-stage embryos were cultured in 4-well NUNC slides in 100% rat serum or DRH medium (50% rat serum, 25% human cord serum and 25% DMEM) until early somite stage. MS-stage embryos were cultured in wells in 100% rat serum or DRH medium until early somite stage or in wells for the first 24 hours followed by roller culture to the early somite stage in DR75. 0B/EB-stage recipient embryos were roller cultured in DR75 medium at 37°C, 5% CO_2 until early somite stage.

Analysis of transgene expression

After culture, embryos containing *lacZ*-expressing cells were fixed for 5 minutes in 4% paraformaldehyde followed by staining overnight at 37°C in X-gal-staining solution. Stained embryos were refixed in 4% paraformaldehyde, photographed and processed for wax histology. 8 μm sections were counterstained with Nuclear fast red. For detection of GFP expression, embryos were fixed in 4% paraformaldehyde overnight at 4°C and examined under a Leica MZFLIII dissecting microscope equipped with a GFP 2-filter set (absorbance peak of 480 nm) or a Leica fluorescent compound microscope with FITC filter set (absorbance peak of 495 nm). Some embryos were split along the midline of the head folds and flat-mounted for microscopy. The specimen was put on a glass slide in a drop of PBS and a coverslip with four Blue-Tac feet was applied to flatten the embryo. Bright-field and fluorescent images were captured using a SPOT 2 digital camera (Scitech, Melbourne, VIC), first as a colour bright-field image then as a monochrome high-resolution fluorescent image. The two images were then painted digitally and superimposed to show the location of the GFP-expressing cells in the embryo, using Photoshop 5.0 (Adobe), ImagePro and the software that operates the digital camera.

Cell labeling

Embryos at the three stages of gastrulation were labeled at the sites shown in Figs 2-4 using either a 0.05% solution of DiI (1,1-dioctadecyl-3,3,3′,3′-tetramethylindocarbocyanine perchlorate, Molecular Probes) or DiO (3,3′-dioctadecyloxacarbocyanide perchlorate, Molecular Probes) diluted in 0.3 M sucrose from a 0.5% ethanolic stock solution. A small volume (0.25-0.5 μl) of dye was injected using a fine glass pipette and the same manipulation apparatus as the cell grafting experiments. After culturing to the early somite stage and fixing in 4% paraformaldehyde overnight, embryos were flat mounted as described previously. To prevent the evaporation of the PBS, the coverslip was sealed with nail polish. The distribution of dye-labeled cells was analyzed using a Leica Diaplan confocal microscope. DiI and DiO fluorescence was visualized using a Rhodamine (absorption at 574 nm) and a FITC filter set (adsorption at 495 nm), respectively (Quinlan et al., 1995).

Whole-mount in situ hybridization

RNA in situ hybridization for *T* and *fgf8* gene expression was performed to determine the development of the PS at each of the three gastrulation stages (Fig. 1). The protocol used for in situ hybridization was as described by Wilkinson and Nieto (1993) with the following modifications. The Ampliscribe kit (Epicentre Technologies) was used in conjunction with Dig-11-UTP (Roche) to synthesize RNA probes, SDS was used instead of CHAPS in the hybridization solution

and post-hybridization washes. Only 5× SSC was used in the hybridization solution, while post-hybridization washes were at 70°C and excluded formamide. No RNA digestion was performed after hybridization.

RESULTS

### The regionalization of mesoderm precursors in the PS

The developmental fate of cells in the PS of the gastrulating embryo was analyzed by tracing the distribution of DiI- or DiO-labeled cells and the pattern of tissue colonization displayed by graft-derived *lacZ*- or GFP-expressing cells. The results obtained from the four lineage markers and two fate mapping techniques are generally concordant (Table 1).

In the ES embryo, cells of the newly formed PS (P1, Fig. 2A) contributed to extraembryonic mesoderm and the amnion (Tables 1, 2: P1) with very minor contribution to the vascular and lateral plate mesoderm. Over 90% of the graft-derived cells were found in the yolk sac mesoderm with a minor contribution to the amnion and the allantois and the same results were obtained for dye-labeled cells (Table 1: P1; Fig. 2D-G). Cells in the anterior proximal epiblast (site A), which will be recruited to the posterior segment of the PS at the MS stage (Lawson et al., 1991), contributed almost exclusively to the extraembryonic mesoderm (Table 1; Fig. 2B,C) with contribution to the allantoic, vascular and lateral plate mesoderm.

In the MS embryo, three different sites in the PS (P2, P3 and P4, Fig. 3A), which extends to about 2/3 of the length of the embryo (Fig. 1) were tested. Cells in the most posterior site (P2) contributed predominantly to the yolk sac mesoderm and the allantois (Fig. 3B-D) with minor contribution to the heart and PS. Cells in the middle site (P3) colonized the extraembryonic tissues as well as the lateral plate mesoderm, paraxial mesoderm and the heart (Fig. 3E-I). Cells from the P4 site were found mostly in the cranial mesoderm and the heart (Fig. 3J-N) with additional contribution to vascular, lateral plate and yolk sac mesoderm. The number of embryos and the relative proportion of cells colonizing the various embryonic tissues is summarized in Table 1. The results of the present PS-mapping study can be integrated with those of the clonal analysis of epiblast cells (Lawson et al., 1991; Lawson and Pedersen 1992a,b). The 6.75 dpc embryo examined by clonal analysis matches the MS embryo in our study. The posterior proximal epiblast adjacent to P2 (zone V of Lawson et al., 1991) contributes mainly to the extraembryonic mesoderm (similar to P2) as well as the rostral mesoderm of the embryo (P3 in our study). The more distal epiblast cells (zone X of Lawson et al., 1991) contributes to anterior mesoderm (similar to our P4) as well as to axial mesoderm.

In the 0B/EB embryo, cells derived from the posterior P5 and P6 sites contributed predominantly to the allantois, and the rest were found evenly among the yolk sac mesoderm and the lateral plate mesoderm (Fig. 4B-E, F-H; Table 1). P7 cells contributed to most mesodermal lineages with the majority found in the lateral plate mesoderm (Table 1; Fig. 4I-L). Cells from the P8 site colonized the somites (Fig. 4M-P), with minor contribution to the cranial, vascular and lateral plate mesoderm. In significant contrast to the cells of the MS-stage

Fig. 2. Fate mapping of the PS in the ES-stage embryo. (A) Site of cell transplantation and labeling: P1, PS (curved line), A, anterior-lateral epiblast. (B,C) Site A transplantation: (B) *lacZ*- and (C) GFP-expressing graft-derived cells in the posterior yolk sac mesoderm and adjacent allantois of the early-somite-stage embryo. (D-G) Site P1 transplantation and labeling: (D) *lacZ*-expressing and (E) GFP-expressing graft-derived cells that populate the chorionic aspect of the yolk sac away from the region that is colonized by site A epiblast cells, (F) Confocal image of DiI-labeled cells derived from site P1 in a flat mount of the allantois of the early-somite embryo and (G) Site P1 cells that colonize the yolk sac mesoderm and the allantois (insert). Arrows point to graft-derived yolk sac mesoderm cells. Magnification: Scale bar, 100 µm (A), 200 µm (B,D), 200 µm (C,E), 50 µm (F) and 30 µm (G).
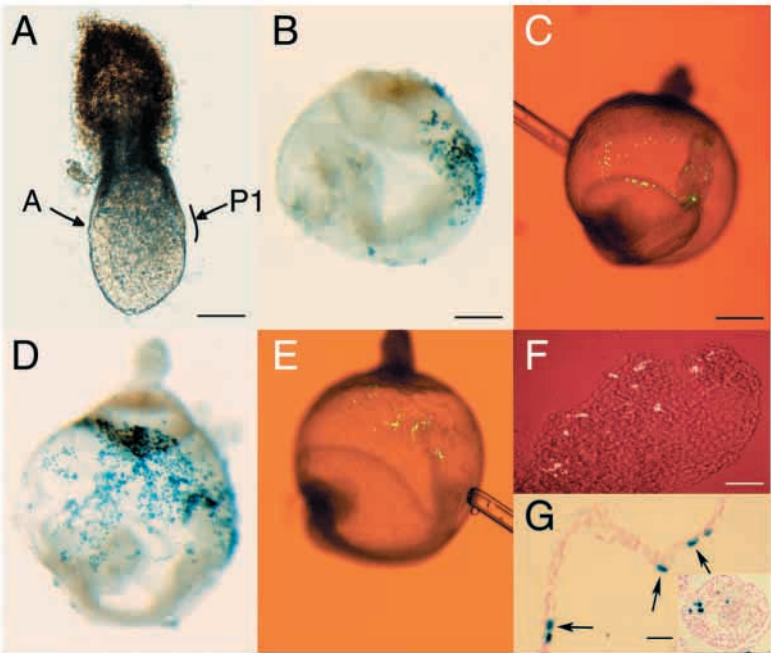
Table 1. The contribution of cells to the embryonic and extraembryonic lineages

| | ES | | | | MS | | | | | | OB/EB | | | | | | | |
| | P1 | | A | | P2 | | P3 | | P4 | | P5 | | P6 | | P7 | | P8 | |
Number/ cell count*	10	2165	12	3047	29	3690	39	3724	35	2107	32	935	10	445	26	559	28	1071
CRM							51%	2.8% (+)‡	66%	65% (++)					8%	4%	18%	1%
HT					7%	2%	51%	14% (++)	51%	22% (++)								
VSL	5%	<1%	8%	<1%			46%	4.2%	46%	4%	16%	4%	20%	5%	18%	6%	18%	10%
AXM									37%						4%	1%	25%	1% (+)
SOM							26%	<1%	34%						27%	11%	89%	79% (+++)
LPM	5%	<1%	8%	<1%			31%	11.7%	26%	4%	40%	15% (+)	50%	68% (++)	81%	61% (+++)	21%	9% (+)
ALL	100%	5% (+)	100%	19% (++)	93%	36% (++)	46%	40.5%			88%	48% (+++)	40%	25.4% (++)	23%	6%		
YSM	100%	94% (+++)	100%	80% (+++)	93%	62% (+++)	46%	26%	5%	5%	88%	18% (+)	40%	0% (+)	4%	1%		
PS					10%	<1%	5%	<1%	3%		66%	15% (+++)	40%	2.5% (++)	46%	10%	29%	0% (+)

Along the top of the table are the three stages studied with the sites tested. The first number for each site represents the percentage of embryos contributing to that site, with the second number being the percentage of *lacZ* expressing cells in each tissue.

*Number of embryos scored for contribution to each lineage (combination of all three techniques)/*lacZ* cell number count at the histological level.

‡GFP-expressing cell contribution from zero to +++ based on colonisation pattern at a whole-mount level. Abbreviations: CRM, Cranial mesoderm; HT, Heart mesoderm; VSL, Vascular endothelium of embryo proper; AXM, Axial mes-endoderm; SOM, Somites; LPM, Lateral plate mesoderm; ALL, Allantois; YSM, Yolk sac mesoderm; PS, Primitive streak.

embryo, there was no contribution by the PS of the 0B/EB embryo to the heart.

Our present analysis has focused on contribution of PS-derived cells to the mesoderm lineages. We have observed only a rare contribution by the PS cells to the gut endoderm. This is primarily because the sites we tested did not include the most anterior segment of the PS at MS or 0B/EB stage. Previously, fate-mapping studies have shown that the posterior epiblast cells that are destined for gut endoderm are recruited to the anteriormost segment of the PS (Lawson et al., 1991) and from

there they move to the endodermal layer (Tam and Beddington, 1992).

The timing of ingression determines the location of PS-derived cells in the anteroposterior embryonic axis

Paraxial mesoderm

Contribution to cranial mesoderm first occurred in the MS embryo from the middle (P3) and anterior (P4) segments of the PS (Table 1). Descendants of the labeled and transplanted cells

Fig. 3. Fate-mapping the PS in the MS-stage embryo. (A) Embryo showing the three sites (P2, P3 and P4) of orthotopic cell transplantation. (B-D) Site P2 transplantation results showing colonization of (B,C) the posterior yolk sac and (D) the allantois by graft-derived cells (B,D, *lacZ*-transgenic cells in whole mount and histological section and C, GFP-transgenic cells, arrows show yolk sac contribution). Site P2-derived cells colonize the entire length of the allantois (D). The distribution of P2-derived cells in the yolk sac (B,C) is similar to site A-derived cells (Fig. 2B,C), suggesting that some cells ingressing at site P2 at mid-gastrulation are derived from site A in the anterior-lateral region of the proximal epiblast. (E-I) Site P3 transplantation results showing the distribution of (E,F) *lacZ*-transgenic cells and (G,H) GFP-transgenic cells to (E,G) the yolk sac near the anterior region of the embryo (arrows in G) and (F,H) the heart and cranial mesoderm of the hindbrain (arrows in H). (I) Section of the host embryo showing colonization of the myocardium of the heart tube by *lacZ*-expressing cells. (J-N) Site P4 transplantation results showing colonisation by (J,K,N) *lacZ*-transgenic and (L,M) GFP-transgenic cells in the cranial mesoderm of the hindbrain and the paraxial mesoderm and lateral mesoderm of the body. (K) The colonization of *lacZ*-transgenic cells in the caudal part of the heart. (L) Bilateral distribution of P4-derived cells in the mesoderm of the hindbrain and the first 2 somites. (N) The presence of graft-derived cell in the cranial mesoderm at the mid-brain level. (I) Anterior-ventral is to the bottom; (L,N) anterior is to the top; (C,D-H,J,K,M) anterior is to the left. Magnification: scale bar, 200 μm (B,C,J), 150 μm (E-H,K-M), and 50 μm (D,I,N).
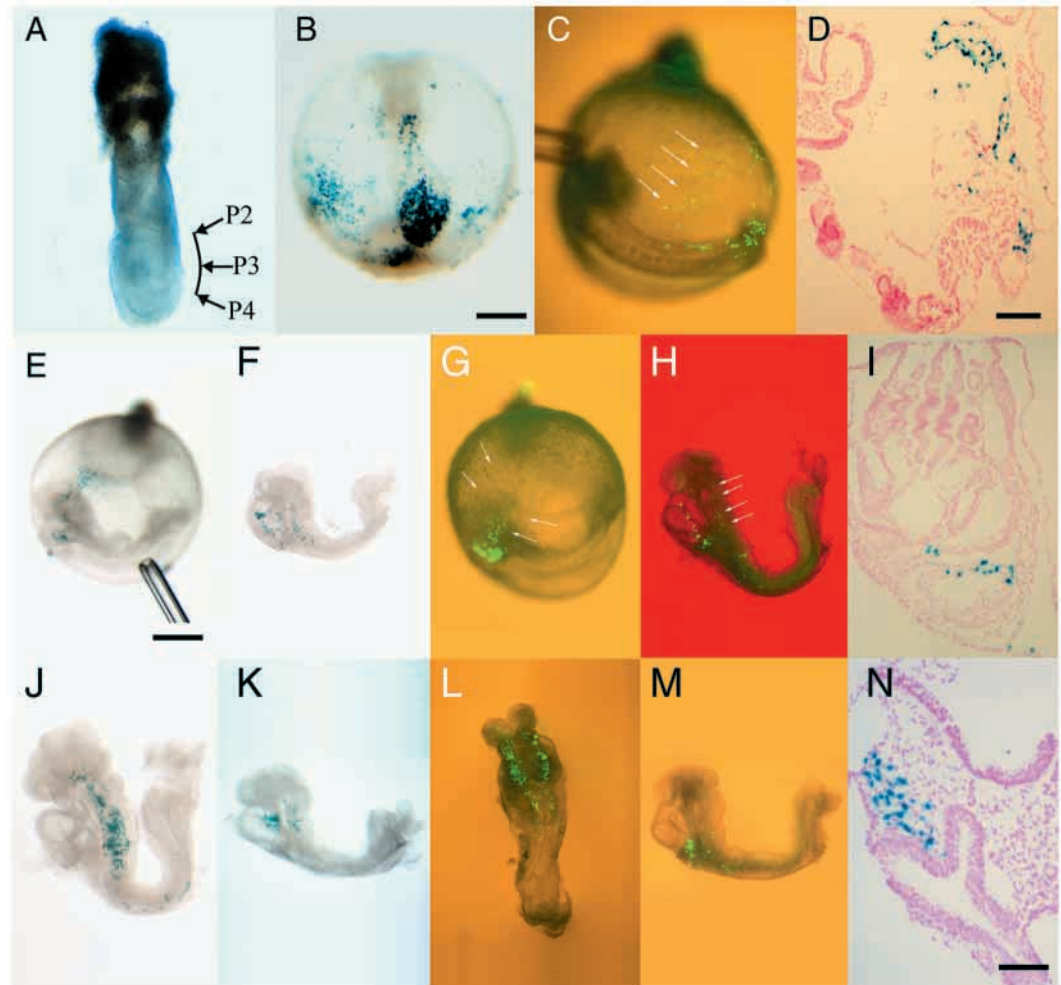
from the P3 site were found in the cranial mesoderm of the midbrain and hindbrain (Fig. 3E-H). Cells from the P4 site, like the P3-derived cells, contribute to the cranial mesoderm of the midbrain and hindbrain (Fig. 3N) and also to the mesoderm of the forebrain in 3 of 23 embryos. By the 0B/EB stage, the PS contained very few precursors of the cranial paraxial mesoderm (Table 1). This suggests that the main bulk of paraxial mesoderm of the forebrain may have exited the PS between the ES and the MS stage as the PS cells of the MS to 0B/EB embryo contributed mainly to the more posterior cranial mesoderm.

At the ES stage, no precursors of the somitic mesoderm were found in the PS. By the MS stage, the middle (P3) and distal (P4) segments made minor contribution to the first 3-4 pairs of somites, in addition to the cranial mesoderm (Table 1). In the 0B/EB embryo, cells derived from the anterior segment (P8) of the PS (Table 1) made major contribution to the somites (Fig. 4M-P). Labeled and transgenic cells colonized both the dermamyotome and the sclerotome of the somites. In the majority of embryos, significant contribution of P8-derived cells began usually with the 4th somite and extended to the rest

of the paraxial mesoderm including the unsegmented presomitic mesoderm. This suggests that the precursors for the first 3-4 somites are allocated to the paraxial mesoderm between the MS and the 0B/EB stage and the PS of the 0B/EB embryo contains the precursors of more posterior somites. This is consistent with the previous finding that ablation of the distal segment of the PS of the 0B/EB embryo leads to the loss of somites that are posterior to the first 3-4 somites (Tam et al., 1999).

In summary, the results for paraxial mesoderm show that the cranial mesoderm of the rostral brain segments ingresses through the streak earlier than the cranial mesoderm of the caudal brain segments and the somitic mesoderm. Results of this and previous studies (Tam and Beddington, 1986, 1987; Tam and Tan, 1992) show that contribution to the trunk somites by the PS begins at late gastrulation and continues through early organogenesis.

Heart mesoderm and lateral plate mesoderm

Heart mesoderm precursors were first present in the PS at the

Fig. 4. Fate mapping of the PS of the late gastrula. (A) The 0B/EB-stage embryo showing the four sites (P5, P6, P7 and P8) of the PS. (B-E) P5 cells colonize the posterior mesoderm of the trunk and the base of the allantoic outgrowth. (B) *lacZ*-transgenic cells in the base of the allantois. (C) GFP-expressing graft-derived cells in the allantois and posterior embryo. (D) Longitudinal section and (E) confocal image of the allantoic bud showing the congregation of *lacZ*-transgenic and DiI-labeled cells, respectively, at the base of the allantois. (F-H) Results of P6 transplantation showing colonization of (F) the presomitic mesoderm and the posterior lateral plate mesoderm and (G,H) the base of the allantoic bud and the posterior embryonic mesoderm. (I-L) Results of P7 transplantation showing the colonization of lateral plate mesoderm (I,K) *lacZ*-transgenic cells, (J) GFP transgenic cells and (L) DiI-labeled cells. (M-P) Results of P8 transplantation showing colonization of the paraxial mesoderm (somites and cranial part of the presomitic mesoderm) of the host embryo by (M,O) *lacZ*-transgenic cells, (N) GFP transgenic cells and (P) DiI-labeled P8 cells. (K,O) Transverse sections. (E,L,P) Flat-mounted specimens visualized by confocal microscopy. Abbreviations: al, allantois; ht; heart; hf; head folds; nt, neural tube; som, somites. Magnification: Scale bar, 100 μm (B,C,G) 50 μm (D,E,H), 200 μm (F,I,J,M,N), 50 μm (K,O); 50 μm (L,P).
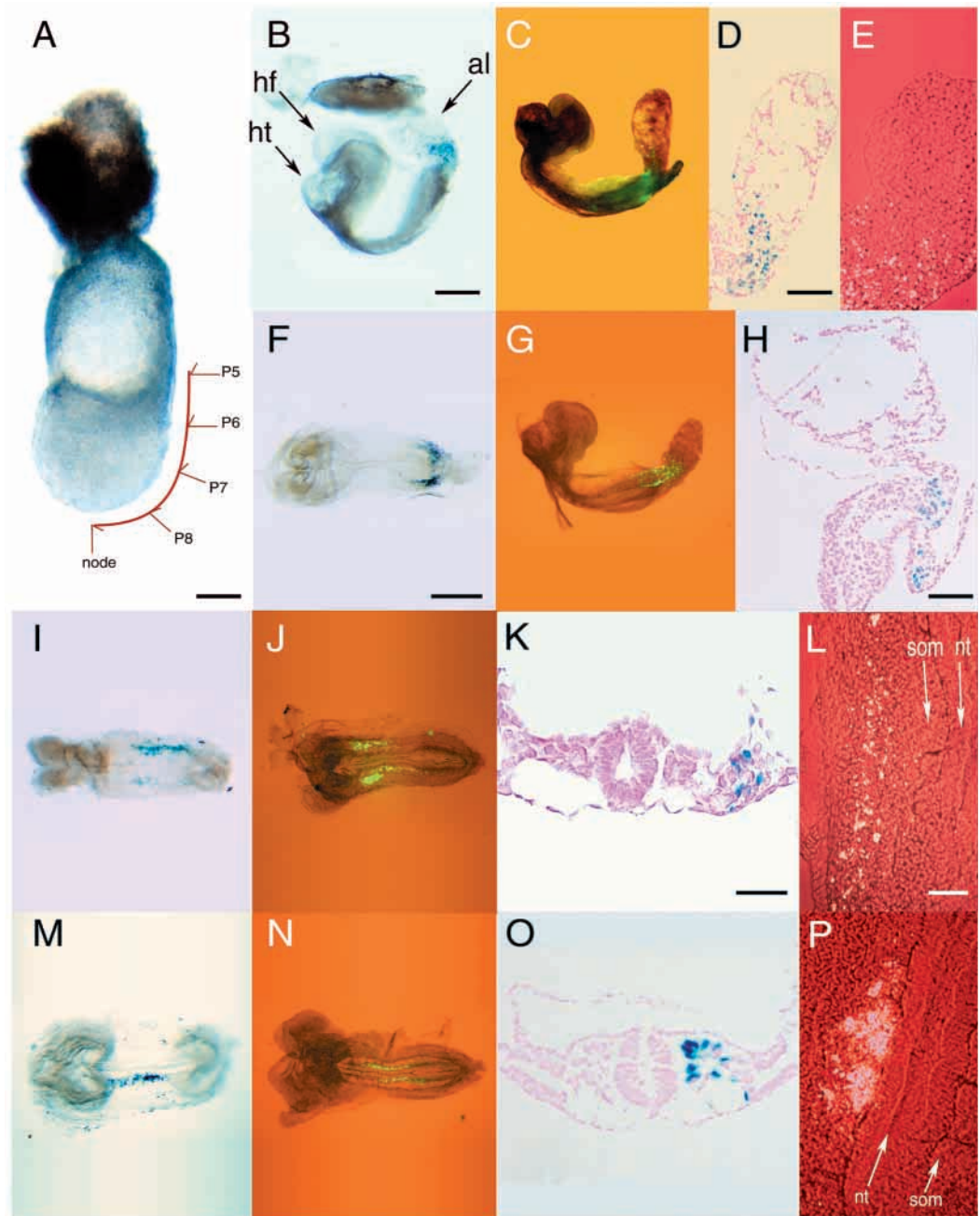

MS stage (Fig. 3E-I,K,M). Precursors of the heart were mapped to the middle (P3) and distal (P4) segments of the PS among the precursors of the cranial mesoderm. Heart precursors were absent from the PS at early and late gastrulation.

Precursors of the lateral plate mesoderm were also mapped to the same sites as the heart mesoderm in the MS-stage PS. More cells from the P3 site than the P4 site colonized the lateral plate mesoderm (Table 1). The streak-derived cells were distributed along the entire length of the lateral mesoderm. Histological analysis showed that streak-derived cells were found in both the splanchnopleure and the somatopleure and, in some embryos, also in the presumptive intermediate mesoderm in the trunk region. By the 0B/EB stage, precursors for the lateral plate

mesoderm were found mainly in the two intermediate segments (P6 and P7) of the PS (Table 1; Fig. 4I-L).

The different timing of recruitment of the extraembryonic blood island cells and vascular progenitors

In the ES embryo, cells from the PS (P1) and the proximal epiblast (A) contributed to the endothelium lining the vitelline vessels in the yolk sac and the blood islands in the vitelline vessels (Fig. 5C,D). The streak, however, preferentially contributed to the erythrocyte precursor cells (Table 2) of the blood islands. Similar dual contribution to endothelium and blood cells was seen for cells derived from the posterior sites (P2 and P3) of the MS-stage PS, but at this stage contribution
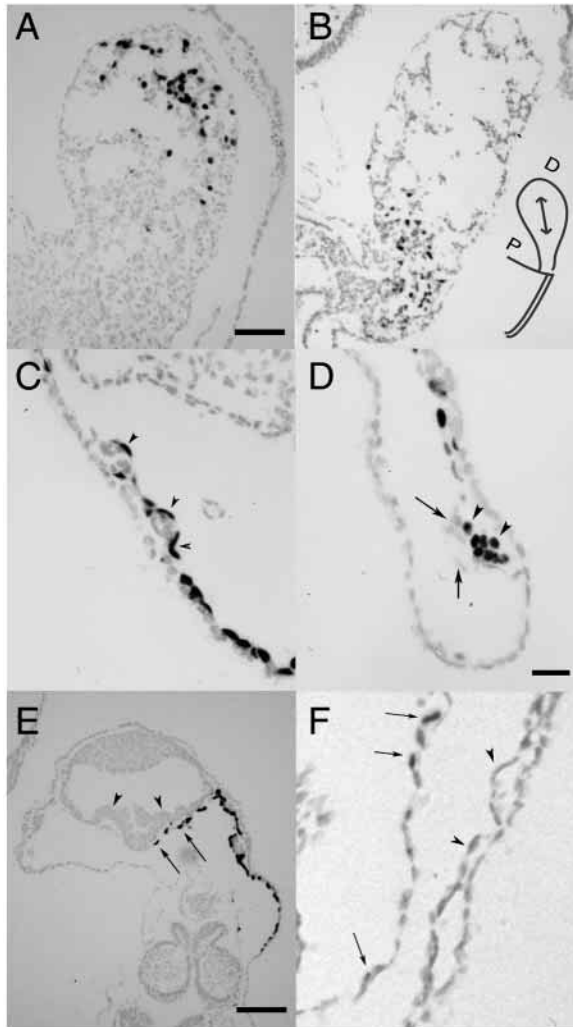
Fig. 5. The contribution of PS (PS) cells to the extraembryonic mesoderm. (A) P2-derived cells in the distal part (the chorionic pole) of the allantois in contrast to (B) P5-derived cells in the proximal part (the base) of the allantois. The insert shows the proximal (P)-distal (D) axis of the allantois. (C) Distribution of PS-derived cells (arrowheads) in the endothelium of the vitelline blood vessels (from site A) and (D) the erythropoietic cells of the blood islands of the yolk sac (from site P1). (D) Note the contrasting size and shape of the erythropoietic cells (arrowheads) and the endothelium (arrows). (E) PS-derived cells (arrows) colonizing the extraembryonic mesoderm associated with the chorion (arrowheads) of the ectoplacental cone. (F) PS-derived cells (arrows) colonizing the amnion, arrowheads point to the yolksac mesoderm. Magnification: Scale bar, 50 µm (A,B), 30 µm (D,C,F), 150 µm (E).

the majority of the blood islands occurs mainly early in gastrulation but contribution to the vascular endothelium is maintained from ES to the 0B/EB stage (Table 2). Simultaneous contribution to blood islands and the vitelline endothelium at the same location in the yolk sac mesoderm was rarely seen. This may suggest that cells that are recruited to these two lineages at different stages of gastrulation, are spatially segregated during the morphogenesis of the vitelline vessels.

### Localization of the PS-derived cells in the extraembryonic tissue correlates with the timing of ingression

Results of the initial analysis show that PS cells of the P1 site in the ES embryo, P2 and P3 sites in the MS embryo and P5 site in the 0B/EB embryo are the major sources of the extraembryonic tissues (Table 1). To discern if there is a regional segregation of the precursors for extraembryonic ectodermal and mesodermal tissues, a more detailed analysis of the contribution of the PS to specific types of extraembryonic tissues was performed (Table 2). Since previous studies have shown that, besides the PS, the proximal epiblast of the ES embryo is also a major source of extraembryonic tissues (Lawson et al., 1991; Lawson and Hage, 1994; Parameswaran and Tam, 1995; Tam and Zhou, 1996), we have also tested cells in the anterior part of the proximal epiblast (Fig. 2A) in the present series for developmental fate.

was mainly to the endothelium with little contribution to erythrocyte precursors (Table 2). Site P4 cells also made minor contribution to the endothelium but no contribution to erythropoietic cells. Cells at site P5 of the 0B/EB embryo only gave rise to endothelial cells of the vitelline vessels (Table 2, P5). Our results show that the allocation of precursor cells to

Table 2. The contribution of cells from the primitive streak and the proximal epiblast to the extraembryonic mesoderm and the amnion of the early-somite-stage embryo

Stage	Site	No. of embryos	Total cell number*	Chorion	Blood islands	Vitelline endothelium	Allantois	Amnion
ES	P1	9	2165	5%	**67%**	23%	4.5%	7%
	A	7	3047	13%	22%	**42%**	19.5%	2.4%
MS	P2	11	3690	5%	4%	**48%**	36%	6%
	P3	5	3724	0%	0.3%	13.6%	**40.5%**	0%
	P4	4	2107	0%	0%	4.6%	0%	0%
OB/EB	P5	11	935	0%	0%	18%	**48%**	0%
	P6	5	445	0%	0%	0%	**25.4%**	0%
	P7	7	559	0%	0%	0%	0%	0%
	P8	7	1071	0%	0%	0%	0%	0%

The contribution of *lacZ*-expressing cells to the extraembryonic mesodermal lineages from each site was analyzed histologically. The percentages in this table represents the fraction that colonizes the extraembryonic mesoderm and amnion only. Bold type indicates the highest contribution for cells originating from each site. Colonization of the various extraembryonic lineages occurs in a lineage-specific manner with the erythrocyte precursors found in the streak early, the vascular endothelium next and finally the majority of cells colonizing the allantois.

*Total number of graft-derived cells in recipient embryos for each site grafted.
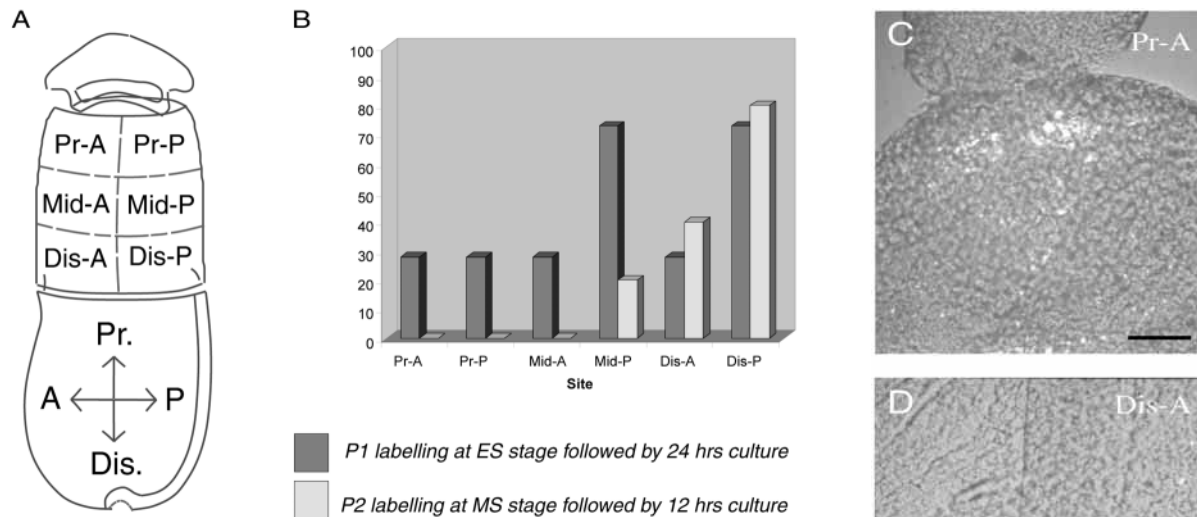
Fig. 6. The anteroposterior and proximodistal colonization of the yolk sac mesoderm. (A) A schematic diagram of the late allantoic bud-stage embryo, showing the embryonic axes and the six compartments for mapping cell distribution in the yolk sac mesoderm. The distribution of P1- and P2-derived cells is mapped after DiI or DiO labeling at the ES and MS stages, respectively. (B) The relative abundance (% of total cell population) in the yolk sac compartments of the late bud-stage embryo, showing more P1-derived cells colonizing the proximal and anterior compartments than P2-derived cells. (C,D) Examples of dye-labeled (C) P1 descendants in the proximal-anterior yolk sac and (D) P2 descendants in the distal-anterior yolk sac. Abbreviations: Pr, proximal; Mid, middle; Dis, distal; A, anterior, P, posterior. (C,D) Proximal side is to the top of the figure. Magnification: scale bar, 50 μm (C,D).

Yolk sac mesoderm

Cells ingressing at the posterior segments of the PS (P1 of the ES embryo and, P2 and P3 of the MS embryo) contributed extensively to the mesoderm lining the visceral yolk sac of the early-somite-stage embryo. Descendants of cells in the anterior epiblast (site A of the ES embryo) also contributed to the extraembryonic mesoderm of the yolk sac and allantois (Fig. 2B,C; Table 1). By following the displacement of the GFP-expressing cells in the cultured embryo, the anterior epiblast cells of the ES embryo were found to be displaced posteriorly and some were incorporated into the PS of the MS embryo (data not shown). The anterior epiblast contributed to the mesoderm of the posterior part of the yolk sac closer to the amnion and the allantois than those from the P1 site of the ES stage PS (compare Fig. 2B,C with D,E). The position of P1 descendants overlapped with the P2-derived population (Fig. 3B). At the MS stage, cells from the P2 and P3 sites were distributed to the allantoic and amnionic side of the yolk sac and by the 0B/EB stage, PS cells colonized the most posterior and distal (amnionic) part of the yolk sac mesoderm.

The shift in distribution of PS-derived cells towards the posterior and distal domains of the yolk sac during development suggests that the chronological order of ingression directly influences the placement of the yolk sac tissues. To compare the fate of the mesodermal cells that ingress at different times of gastrulation, cells in the posterior PS of the ES and MS embryo were labeled in situ with DiI or DiO and the localization of the labeled cells was mapped in the yolk sac after culture to the late bud stage in vitro (Fig. 6A). Cells from the ES-stage PS were found in the entire yolk sac including the most proximal (the chorionic aspect) region (Fig. 6B,C). In contrast, cells from the MS-stage PS were only found in the intermediate and the

amnionic aspect of the yolk sac (Fig. 6B,D). These results demonstrate that at the ES-stage mesodermal progenitors for the entire yolk sac are present in the streak but, by the MS stage, the PS contains only the distal and posterior yolk sac precursors. These results, in conjunction with a similar change in distribution of graft-derived *lacZ* or GFP-transgenic cells from the PS of the ES and MS embryo (Figs 2D,E, 3B,C) show that the yolk sac mesoderm is recruited in a sequential order from the chorionic to the amnionic compartment.

Allantois

Significant contribution by the PS to the allantois began at the MS stage and continued to the 0B/EB stage. Prior to the MS stage, the posterior PS only made a minor contribution to the allantois (Tables 1, 2). Only a small number of P1 cells were found in the allantois but they were distributed throughout the length of the allantois (Fig. 2D-F). In contrast, the proximal epiblast cells, which will be recruited later to the P2 segment of the MS embryo, contributed more extensively to the allantois than the P1 population (Fig. 3B). Cells at the P2 site of the MS embryo were found in the entire allantois with a preponderance to the more distal part that later fuses with the chorion (Fig. 3B-D). At the 0B/EB stage, the P5 segment of the PS was the major source of allantoic mesoderm (Fig. 4B-E). These streak-derived cells, in contrast to those that ingressed earlier (Fig. 5A), were localized to the base of the allantois (Fig. 5B). These results are consistent with those of Downs and Harmann (1997) on sequential recruitment of cells to different parts of the allantois at late gastrulation.

Mesoderm of the chorion

The mesodermal cells lining the yolk sac surface of the chorion (Fig. 5E) were derived from the PS and the proximal epiblast

of the ES embryo, and the P2 site in the PS of the MS embryo (Table 2). The PS of the 0B/EB embryo did not contain any chorionic mesoderm precursors. This is consistent with the view that cells reaching the most distant sites of the extraembryonic membranes have to ingress earlier during gastrulation. The streak-derived cells never colonized the ectodermal tissue of the chorion, which is derived from the extraembryonic ectoderm (Rossant et al., 1986; Tam, unpublished).

Amnion

Contribution to the amnion (both mesoderm and ectoderm components) was seen only from sites P1 and A in the ES embryo and P2 in the MS-stage embryo (Fig. 5F; Table 2).

DISCUSSION

Regionalization of cell fates in the PS and the timing of allocation of mesodermal lineages to the anteroposterior embryonic axis

By using a combination of four different lineage markers and two separate fate-mapping techniques, we have established detailed fate maps of the PS at three stages of gastrulation (Fig. 7). These maps depict a dynamic change in the cellular composition of the PS and reveal the order in which different mesodermal lineages are established during gastrulation. The fate maps of the PS of the mouse gastrula are remarkably similar to those of the avian embryo at comparable stages of gastrulation (Fig. 7; reviewed by Tam et al., 1999).

Clonal analysis of the developmental fate of epiblast cells has shown that there is little correlation between the position of the cells in the epiblast and the distribution of their descendants in the ectodermal or mesodermal derivatives in the anteroposterior axis of the embryo (Lawson et al., 1991; Lawson and Pedersen 1992a,b). However, a more distinct regionalization along the anteroposterior axis is found for cells derived from the PS at different stages of gastrulation (Fig. 8). This suggests that cells may become spatially restricted following ingression and the order in which this movement takes place has a direct influence on the location of the cells in the body plan. Indeed mapping of the developing mesoderm has shown that cells within the mesodermal wing show regionalization of precursors which may be correlated with the order of allocation of the ingressed cells to the germ layer (Parameswaran and Tam, 1995; Tam et al., 1997). When the location of the PS-derived cells in the paraxial and lateral mesoderm is mapped for the different sites and stages, it becomes apparent that cells derived from the PS of the MS embryo contribute preferentially to the mesodermal tissues in the more rostral part of the embryo than those of the 0B/EB stage. The anteroposterior pattern of mesoderm tissues is therefore established according to the temporal order of cell recruitment (Fig. 8). Allocation of the PS cells to the mesoderm may be concomitant to a restriction in lineage potency. This has been demonstrated by the inability of recently ingressed mesodermal cells to colonize the lateral mesoderm after they are transplanted back to the epiblast for another round of gastrulation (Tam et al., 1997).

### The temporal and spatial order of recruitment of tissue progenitors to the yolk sac mesoderm

The discovery that the progenitors of the blood island cells and endothelial cells of the yolk sac may be allocated at different times and that a simultaneous contribution by PS-derived cells to the two tissue lineages in the same region of the yolk sac is seldom encountered raises the possibility that during early gastrulation these two cell lineages may arise from different progenitor populations. The early allocation of the erythropoietic cells may account for the early expression of transcription factors that herald erythropoiesis such as *rbtns* and *tal1* (Shivdasani et al., 1995; Warren et al., 1994) in the extraembryonic mesoderm of the MS embryo (Silver and Palis, 1997). Molecular markers associated with vasculogenesis such as *Flk1* are expressed in the extraembryonic mesoderm at the late gastrulation stage (Yamaguchi et al., 1993; Dumont et al., 1995) as would be expected based on the timing of ingression. *Flt-1*, a gene associated with vasculogenesis, is expressed at the early- to mid-streak stage in the region of the blood islands and shows upregulation as the embryo develops becomes endothelium-specific by the early somite stage (Fong et al., 1996). The close correlation between the timing of ingression of endothelial precursors and gene upregulation suggests that *Flt-1* is the earliest marker of presumptive vitelline endothelial cells.

Results of the present study show that mesodermal tissues of different extraembryonic structures are recruited at different stages of gastrulation. The progenitors of the yolk sac mesoderm are found in the PS earlier in gastrulation than those of the allantoic mesoderm as expected (Lawson et al., 1991). Within the yolk sac, progenitors destined for the more chorionic aspect of the yolk sac are present in the streak ahead of those destined for a more amnionic aspect. In the allantois, cells destined for the more distal part of the allantoic bud that later fuses with the chorion (Downs and Gardner, 1995), emerge from the PS of the MS embryo while those for the basal part of the allantois are recruited from the PS of the late-streak to 0B/EB embryo (Downs and Harmann, 1997 and this study).

The translation of the epiblast fate map to the final body plan

Previous fate-mapping studies have demonstrated that cells in different regions of the epiblast of the early gastrula display diverse developmental fates, suggesting that the progenitor population for various fetal and extraembryonic tissue lineages may be spatially segregated prior to germ layer formation (reviewed by Lawson and Pedersen, 1992a,b; Tam and Behringer, 1997). However, with the exception of the neuroectodermal progenitors (Quinlan et al., 1995), there is no distinct or predictable predisposition of the descendants of the mesodermal and endodermal progenitors in the anteroposterior, dorsoventral and lateral embryonic axes (Lawson et al., 1991; Lawson and Pedersen, 1992a,b; Tam and Behringer, 1997; Tam et al., 1997). The analysis of developmental fate of cells in the PS of the late mouse gastrula has revealed that cells ingressing through different anteroposterior segments of the PS are allocated respectively to mesodermal tissues in specific dorsoventral locations of the fetal body (Tam and Beddington, 1987; Smith et al., 1994). Furthermore, it has been shown that the allocation of the mesodermal tissues to the somites and the endodermal cells to the fetal gut follows a craniocaudal order that may be related to the time that the cells emerge from the PS during gastrulation and early organogenesis (Lawson et al., 1986,
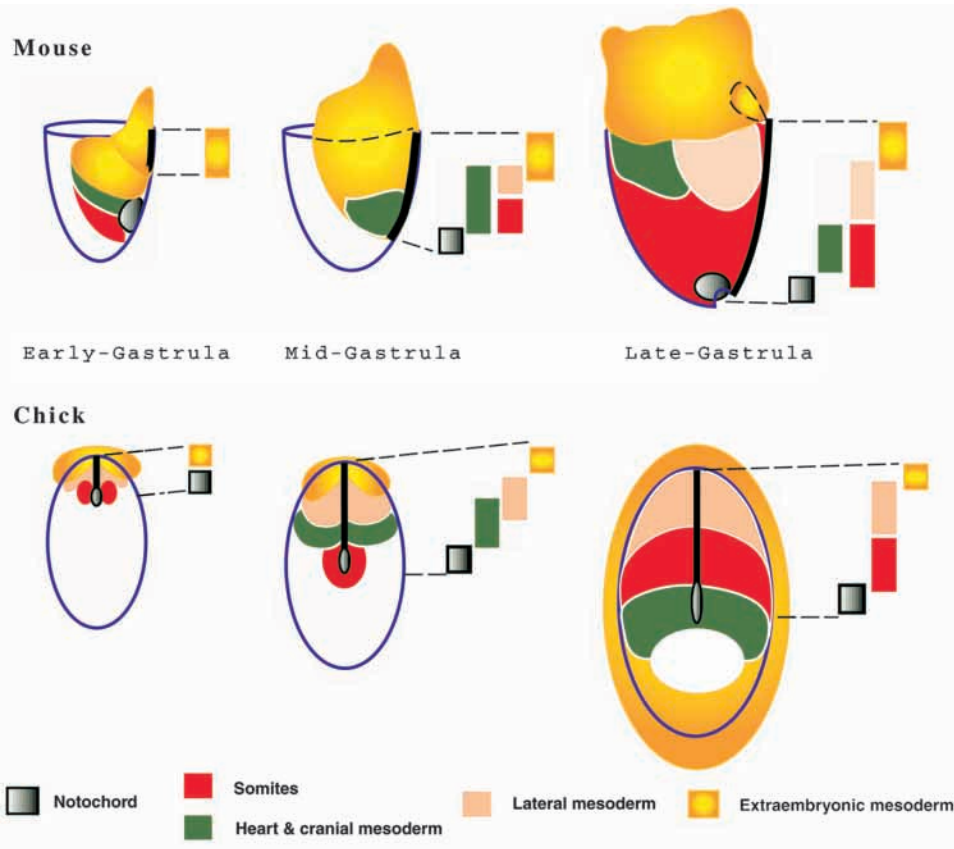
Fig. 7. The similarity in the developmental fates of cells in the PS of the mouse and avian gastrulae. Coloured bars next to the PS represent the regionalization of different mesodermal precursors in the PS. The location of the mesodermal progenitors in the epiblast is shown for the early-streak-stage embryo of both species and only the location of the somite precursors in the epiblast is shown for the MS avian embryo. The lineage composition of the mesodermal layer is shown in an overlay on the epiblast for the three stages of gastrulation. The anterior side of the mouse gastrula is facing towards the left (top) and that of the avian gastrula towards the bottom of the figure to allow the parallel alignment of the PSs.

1991; Lawson and Pedersen, 1987, 1992a,b; Tam and Beddington, 1986, 1987, 1992). These findings have therefore highlighted the morphogenetic impact of the order and site of ingression of the epiblast-derived cells during gastrulation to the spatial allocation of mesodermal and endodermal progenitors. Results of our study have extended this concept to the extraembryonic mesodermal lineages and to other mesodermal tissues in addition to the somites, and demonstrate that the translation of the fate map in the epiblast into the final body plan is accomplished by regulating the order and timing of the transit of the precursor cells through the PS during gastrulation.
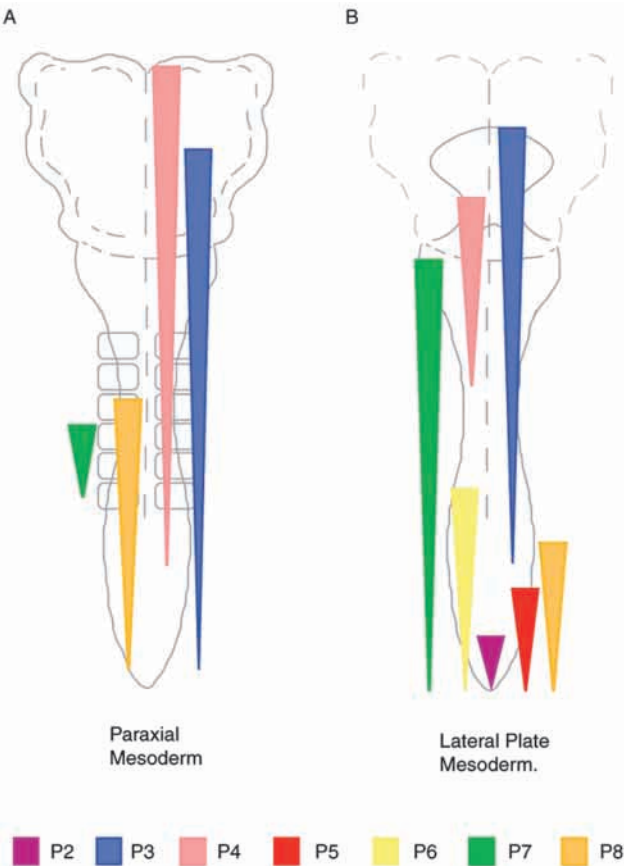
Fig. 8. Distribution of PS-derived cells in the mesodermal tissues along the anteroposterior axis. P2, P3 and P4 are sites in the PS of the MS embryo and P5, P6, P7 and P8 are in the PS of the 0B/EB embryo. Each colour-coded triangular bar represents the distribution of cells from a specific site in the PS. (A) Contribution of descendants to the paraxial mesoderm in the cranial region and the trunk of the early-somite-stage embryo. Only graft-derived or labeled P4 cells of the MS embryo are found in the mesoderm at the forebrain level, but both P3 and P4 cells contribute the paraxial mesoderm of the midbrain and hindbrain. Cells from the anterior parts of the PS (P7 and P8 sites) of the late gastrula contribute to paraxial mesoderm posterior to the 3rd-4th somites, suggesting that the precursors for the first 2-3 somites have ingressed through the streak between the MS and 0B/EB stage. (B) Distribution of graft-derived cells and labeled PS cells to the lateral plate mesoderm and heart mesoderm of the early-somite-stage embryo. The most extensive contribution to the lateral plate mesoderm is made by P3 cells of the MS embryo and P7 cells of the 0B/EB embryo. Only cells in the PS of the MS embryo contribute to the heart mesoderm.

REFERENCES

Downs, K. M. and Davies, T. (1993). Staging of gastrulating mouse embryos by morphological landmarks in the dissecting microscope. *Development* **118,** 1255-1266.

Downs, K. M. and Gardner, R. L. (1995). An investigation into early placental ontogeny: allantoic attachment to the chorion is selective and developmentally regulated. *Development* **121,** 407-16.

Downs, K. M. and Harmann, C. (1997). Developmental potency of the murine allantois. *Development* **124,** 2769-80.

Dumont, D. J., Fong, G.-H., Puri, M. C., Gradwohl, G., Alitalo, K. and Breitman, M. L. (1995). Vasculization of the mouse embryo: a study of *flk-1, tek, tie* and Vascular Endothelial Growth Factor expression during development. *Dev. Dyn.* **203,** 80-92.

Fong, G.-H., Klingensmith, J., Wood, C. R., Rossant, J. and Breitman, M. L. (1996). Regulation of *Flt-1* expression during mouse embryogenesis suggests a role in the establishment of vascular endothelium. *Dev. Dyn.* **207,** 1-10.

Gardner, R. L. and Cockroft, D. L. (1998). Complete dissipation of coherent clonal growth occurs before gastrulation in mouse epiblast. *Development* **125,** 2397-402.

Hadjantonakis, A-K., Gertsenstein, M., Ikawa, M., Okabe, M., and Nagy, A. (1998). Generating green fluorescent mice by germline transmission of green fluorescent ES cells. *Mech. Dev.* **76,** 79-90.

Hashimoto, K., Fujimoto, H. and Nakatsuji, N. (1987). An ECM substratum allows mouse mesodermal cells isolated from the primitive streak to exhibit motility similar to that inside the embryo and reveals a deficiency in the T/T mutant cells. *Development* **100,** 587-98.

Kinder, S. J., Tan, S.-S. and Tam, P. P. L. (1999). Cell grafting and fate mapping of the early-somite-stage mouse embryo. *In Methods in Molecular Biology: Developmental Biology Protocols Volumes I and II*. Humana Press Inc. Chapter 29a. *In Press*.

Lawson, K. A. and Hage, W. J. (1994). Clonal analysis of the origin of primordial germ cells in the mouse. *Ciba Found Symp*. **182,** 68-84.

Lawson, K. A. and Pedersen, R. A. (1987). Cell fate, morphogenetic movement and population kinetics of embryonic endoderm at the time of germ layer formation in the mouse. *Development* **101,** 627-652.

Lawson, K. A. and Pedersen, R. A. (1992a). Clonal analysis of cell fate during gastrulation and early neurulation in the mouse. *Ciba Found Symp* **165,** 3-21.

Lawson, K. A. and Pedersen, R. A. (1992b). Early mesoderm formation in the mouse embryo. In *Formation and Differentiation of Early Mesoderm*. (ed. Bellairs, R., Sanders, E. J. and Lash, J. W). New York: Plenum Press.

Lawson, K. A., Meneses, J. J. and Pedersen, R. A. (1986). Cell fate and cell lineage in the endoderm of the presomite mouse embryo, studied with an intracellular tracer. *Dev. Biol.* **115,** 325-339.

Lawson, K. A., Meneses, J. J. and Pedersen, R. A. (1991). Clonal analysis of epiblast fate during germ layer formation in the mouse embryo. *Development* **113,** 891-911.

Nishikawa, S. I., Nishikawa, S., Hirashima, M., Matsuyoshi, N. and Kodama, H. (1998). Progressive lineage analysis by cell sorting and culture identifies FLK1+VE-cadherin+ cells at a diverging point of endothelial and hemopoietic lineages. *Development* **125,** 1747-1757.

Parameswaran, M. and Tam, P. P. L. (1995). Regionalisation of cell fate and morphogenetic movement of the mesoderm during mouse gastrulation. *Dev. Genet.* **17,** 16-28.

Quinlan, G. A., Williams, E. A., Tan, S.-S. and Tam, P. P. L. (1995). Neuroectodermal fate of epiblast cells in the distal region of the mouse egg cylinder: Implication for body plan organization during early embryogenesis. *Development* **121,** 87-98.

Rossant, J., Sanford, J. P., Chapman, V. M. and Andrews, G. K. (1986). Undermethylation of structural gene sequences in extraembryonic lineages of the mouse. *Dev. Biol.* **117,** 567-73.

Shivdasani, R. A., Mayer, E. L. and Orkin, S. H. (1995). Absence of blood formation in mice lacking T-cell leukemia oncoprotein tal-1/SCL. *Nature* **373,** 432-34.

Silver, L. and Palis, J. (1997). Initiation of murine erythropoiesis: A spatial analysis. *Blood* **89,** 1154-1164.

Smith, J. L., Gesteland, K. M. and Schoenwolf, G. C. (1994). Prospective fate map of the mouse primitive streak at 7. 5 days of gestation. *Dev. Dyn.* **202,** 279-289

Sturm, K. and Tam, P. P. L. (1993). Isolation and culture of whole postimplantation embryos and germ layer derivatives. *Methods Enzymol.* **225,**164-90.

Tam, P. P. L. and Beddington, R. S. P. (1986). The metameric organization of the presomitic mesoderm and somite specification in the mouse embryo. In *Somites in Developing Embryos* NATO ASI series, (ed. R. Bellairs, J. Lash and D. A. Ede). pp 17-36. New York: Plenum Press.

Tam, P. P. L. and Beddington, R. S. P. (1987). The formation of mesodermal tissues in the mouse embryo during gastrulation and early organogenesis. *Development* **99,** 109-126.

Tam, P. P. L. and Beddington, R. S. P. (1992). Establishment and organisation of germ layers in the gastrulating mouse embryo. In *Post-Implantation development in the mouse*. *Ciba Found. Symp.* **165,** 27-49. New York: Wiley.

Tam, P. P. L. and Behringer, R. R. (1997). Mouse gastrulation: the formation of the mammalian body plan. *Mech. Dev.* **68,** 3-25.

Tam, P. P. L. and Tan, S. S. (1992). The somitogenetic potential of cells in the primitive streak and the tail bud of the organogenesis-stage mouse embryo. *Development* **115,** 703-715.

Tam, P. P. L. and Zhou, S. X. (1996). The allocation of epiblast cells to ectodermal and germ-line lineages is influenced by the position of the cells in the gastrulating mouse embryo. *Dev. Biol.* **178,** 124-132.

Tam, P. P. L., Goldman, D., Camus, A. and Schoenwolf, G. C. (1999). Early events of somitogenesis in higher vertebrates: Allocation of precursor cells during gastrulation and the organisation of a meristic pattern in the paraxial mesoderm. *Curr. Top. Dev. Biol.* **47,** 1-32.

Tam, P. P. L., Parameswaran, M., Kinder, S. J. and Weinberger, R. P. (1997). The allocation of epiblast cells to the embryonic heart and other mesodermal lineages: the role of ingression and tissue movement during gastrulation. *Development* **124,** 1631-1642.

Tam, P. P. L., Williams, E. A. and Chan, W. Y. (1993). Gastrulation in the mouse embryo: ultrastructural and molecular aspects of germ layer morphogenesis. *Microsc. Res. Tech.* **26,** 301-328

Warren, A. J., Colledge, W. H., Carlton, M. B. L., Evans, M., Smith, A. J. H. and Rabbitts, T. H. (1994). The oncogene cysteine-rich LIM domain protein is essential for erythroid development. *Cell* **78,** 45-57.

Wilkinson, D. G. and Nieto, M. A. (1993). Detection of messenger RNA by *in situ* hybridization to tissue sections and wholemounts. *Methods Enzymol.* **225,** 361-373.

Yamaguchi, T. P., Dumont, D. J., Conlon, R. A., Breitman, M. L. and Rossant, J. (1993). *flk-1*, an flt-related receptor tyrosine kinase is an early marker for endothelial cell precursors. *Development* **118,** 489-98.